International Journal of Modern Physics D

Constraints on Cosmological Models with Gamma-Ray Bursts in Cosmology-Independent Way

Hanbei Xie, Xiaodong Nong, Huifeng Wang, Bin Zhang, Zihao Li, and Nan Liang*

Key Laboratory of Information and Computing Science Guizhou Province, Guizhou Normal University, Guiyang, Guizhou 550025, China
School of Cyber Science and Technology, Guizhou Normal University, Guiyang, Guizhou 550025, China
School of Mathematical Sciences,Guizhou Normal University, Guiyang, Guizhou 550025, China
Joint Center for FAST Sciences Guizhou Normal University Node, Guiyang, Guizhou 550025, China
**E-mail:liangn@bnu.edu.cn*

Received Day Month Year
Revised Day Month Year

In this paper, we present a cosmology-independent method to constrain cosmological models from the latest 221 gamma-ray bursts (GRBs) sample, including 49 GRBs from Fermi catalog with the Amati relation (the $E_{\rm p}$-$E_{\rm iso}$ correlation), which calibrated by using a Gaussian process from the Pantheon+ type Ia supernovae (SNe Ia) sample. With 182 GRBs at $0.8 \leq z \leq 8.2$ in the Hubble diagram and the latest observational Hubble data (OHD) by the Markov Chain Monte Carlo (MCMC) method, we obtained $\Omega_{\rm m} = 0.348^{+0.048}_{-0.066}$ and $h = 0.680^{+0.029}_{-0.029}$ for the flat ΛCDM model, and $\Omega_{\rm m} = 0.318^{+0.067}_{-0.059}$, $h = 0.704^{+0.055}_{-0.068}$, $w = -1.21^{+0.32}_{-0.67}$ for the flat wCDM model. These results are consistent with those in which the coefficients of the Amati relation and the cosmological parameters fitted simultaneously.

Keywords: gamma-ray bursts, general - cosmology, observations.

PACS numbers:

1. Introduction

Long Gamma-ray bursts (GRBs) are the most intense and energetic bursts of gamma rays from the cosmic space within a short period of time. Currently, the maximum observable redshift of GRBs is estimated to be around $z = 9.4$,[1] which is significantly greater than Type Ia supernovae (SNe Ia), with the maximum observable redshift $z \sim 2.3$.[2] Several empirical GRB luminosity relations, which are connections between measurable properties of the instantaneous gamma-ray emission and the luminosity or energy, have been proposed to standardize GRBs.[3–13] However, the early studies had usually calibrated the luminosity relations of GRBs by assuming a FIDUCIAL cosmological model.[11,14] Therefore, using these model-dependent GRB data to constrain cosmological models leads to the circularity problem.[10] Liang *et al.*[15] proposed a model-independent method to calibrate the luminosity relations of GRBs with SNe Ia data by the interpolation method and construct the GRB Hubble diagram, which can be used to constrain cosmological models.[16–23] The luminosity relations of GRBs can be calibrated with SNe Ia data by the similar methods.[13, 24–35]

Furthermore, the observational Hubble data (OHD) obtained with the cosmic chronometers (CC) method, which related the evolution of differential ages of passive galaxies at different redshifts,[36, 37] have unique advantages to calibrate GRBs in a model-independent way. Amati *et al.*[38] proposed an alternative method to calibrate GRB correlations by using the OHD through the Bézier parametric curve and built up a Hubble diagram consisting of 193 GRBs with the Amati relation (the $E_{\rm p}$-$E_{\rm iso}$ correlation).[5] Following this method,[38] several works have constrained cosmological models with the Amati relation.[39–42]

On the other hand, the simultaneous fitting method, in which the coefficients of relations and the parameters of the cosmological model are constrained simultaneously, has been proposed to avoid the circularity problem.[43] Khadka *et al.*[44] compile a data set of 118 GRBs (the A118 sample,[45] including 25 Fermi GRB sample[46]) with the smallest intrinsic dispersion from the total 220 GRBs (the A220 sample) with the Amati relation to derive the correlation and cosmological model parameters simultaneously. Cao *et al.*[47–49] used the Amati relation[5] with the A220 and the A118 GRB samples in conjunction with **the Dainotti relation**[a] to constrain cosmological model parameters by the simultaneous fitting method. **They showed that Platinum sample including 50 GRB data can be standardized with a cosmological-model-independent 3D Dainotti relation,[48] and the 3D Dainotti is strongly favoured over the 2D one with different GRB data compilation.[49] Dainotti *et al.*[73, 74] usd optical and X-ray GRB fundamental planes as cosmological distance indicators. Dainotti *et al.*[76] correctted the 3D relation by considering the selection and evolutionary effects with a reliable statistical method to obtain a lower central value for the intrinsic scatter. The 3D Dainotti relation have also been used with a binned analysis with GRBs, SNe Ia, and baryonic acoustic oscillations (BAOs);[75] and joint constraints combined GRBs with quasars, SNe Ia, and BAOs;[77, 78] as well as a robust cosmographic technique.[79]**

[a]**Compared to GRB relations of the prompt emission phase, the relations involving the X-ray afterglow plateau phase[50–52] exists less variability in its features. Dainotti *et al.* proposed the relation between the plateau luminosity and the end time of the plateau in X-ray afterglows (2D Dainotti relation[50]), which have been used to cosmological constraint.[53–59, 62] Furthermore, the GRB Fundamental Plane relation (the 3D Dainotti relation) among the rest-frame time and X-ray luminosity at the end of the plateau emission and the peak prompt luminosity with small intrinsic scatter has been found.[60, 63–65, 67] Some similar 2D and 3D relations with the plateau in the X-ray afterglows has also been found.[70–72] Recently, the relationship in optical wavelengths between the optical rest-frame end time and the optical luminosity at the end of the plateau has been found.[66] Very recently, the GRB relation in radio plateau phase afterglows has also been investigated.[68, 69]**

Up to now, whether the luminosity relations of GRB are redshift dependent or not is still under debate. The possible evolutionary effects in GRB relations have been discussed **in many works[29,30,74,76,80–84]**. **Regarding the luminosity function and density rate and cosmological evolution of the formation rate of GRBs, the luminosity relations of GRB could be evolution with redshift[85–89]**. With the A220 sample, Khadka *et al.*[44] found that the Amati relation is independent of redshift within the error bars; Liu *et al.*[23,90] proposed the improved Amati relation by accounting for evolutionary effects via copula, and found that a redshift evolutionary correlation is favored slightly; Kumar *et al.*[91] divided the GRB data into five distinct redshift bins to calibrate the Amati relation, and found that GRBs do seem to evolve with cosmological redshift.

Recently, Jia *et al.*[92] found no statistically significant evidence for the redshift evolution with the Amati relation from the analysis of data in different redshift intervals with a long GRB sample, which contains 221 long GRBs with redshifts from 0.03 to 8.20, including 49 GRBs from Fermi catalog. Liang *et al.*[35] calibrated the Amati relation with the A219 sample and the A118 sample by using a Gaussian process from the Pantheon samples with 1048 SNe Ia data points,[2] and constrain cosmological models in flat space with GRBs at high redshift and 31 OHD via the Markov Chain Monte Carlo (MCMC) numerical method. Li, Zhang & Liang[93] calibrated GRB from the latest 32 OHD via the Gaussian process to construct the GRB Hubble diagram with the A118 data set, and constrain Dark Energy models with GRBs at high redshift and SNe Ia in a flat space by the MCMC method. More recently, Mu *et al.*[94] reconstruct cosmography parameters up to fifth order with the Amati relation of the A219 sample[35] calibrated from Pantheon+ samples,[95] which contains 1701 SNe light curves of 1550 spectroscopically confirmed SNe Ia at redshift $z < 2.26$.

In this paper, we utilize the latest 221 GRB data compiled in Ref. 92 (the J221 sample) and the Pantheon+ sample[95] to calibrate the Amati relation by Gaussian process at low redshift, and obtained the Hubble diagram of GRBs. We constrain cosmological models with the GRBs at high redshift and the latest 32 OHD data[93] by the MCMC method. Finally, we also use the simultaneous fitting method for constraints on cosmological models.

2. CALIBRATION OF THE AMATI RELATION

The Amati relation,[5] which connects the spectral peak energy and the isotropic equivalent radiated energy (the $E_{\rm p}$-$E_{\rm iso}$ correlation) of GRBs, can be expressed as

$$y = a + bx, \tag{1}$$

where $y = \log_{10}\frac{E_{\rm iso}}{1{\rm erg}}$, $x = \log_{10}\frac{E_{\rm p}}{300{\rm keV}}$, and a and b are free coefficients, $E_{\rm iso}$ and $E_{\rm p}$ can be calculated by

$$E_{\rm iso} = 4\pi d_L^2(z) S_{\rm bolo}(1+z)^{-1}, \quad E_{\rm p} = E_{\rm p}^{\rm obs}(1+z), \tag{2}$$

where $E_{\rm p}^{\rm obs}$ and $S_{\rm bolo}$ are the GRB spectral peak energy and bolometric fluence. It should be noted that the values of $E_{\rm iso}$ from Tab. 1 in Ref. 92 are related with luminosity distance d_L, which depend on cosmological models. The luminosity distance can be calculated by $d_{\rm L}(z) = \frac{c(1+z)}{H_0}\int_0^z \frac{{\rm d}z'}{\sqrt{\Omega_m(1+z')^3+\Omega_\Lambda}}$, where $\Omega_{\rm m}$ represents the parameter for non-relativistic matter density, Ω_Λ represents the cosmological constant density, and H_0 represents the Hubble constant. Jia *et al.*[92] used the standard cosmological parameters from Plank Collaboration[96] ($\Omega_{\rm m} = 0.315$, $\Omega_\Lambda = 0.685$, and $H_0 = 67.4$ km s^{-1} Mpc^{-1}) to obtain the values of $E_{\rm iso}$.

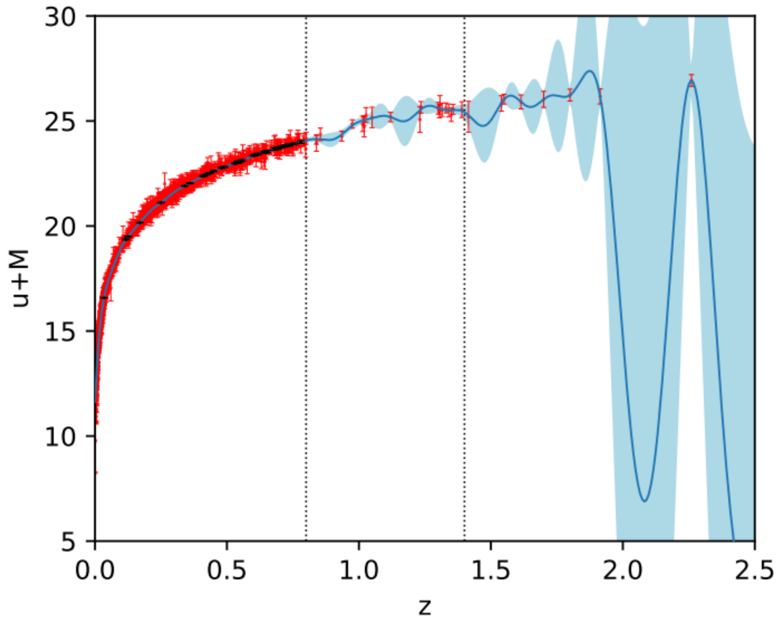

Fig. 1. The apparent magnitudes reconstructed through the Gaussian process from SNe Ia data at $z \leq 2.26$. The blue curves present the reconstructed function with the 1σ uncertainty from the SNe Ia data (red dots). The apparent magnitudes of GRBs at $z < 0.8$ (black dots) are reconstructed from SNe Ia. The dashed line denotes $z = 0.8$ and $z = 1.4$.

Gaussian process is a fully Bayesian method for smoothing data, which can effectively reduce the errors of reconstructed results.[97,98] Recently, Gaussian process has been widely applied to the field of cosmology.[35,71,93,99–102]In order to obtain model-independent $E_{\rm iso}$, we use a Gaussian process to reconstruct the values of the luminosity distance (d_L) of GRBs from SNe Ia data. In the Gaussian process, the function values $f(z)$ are correlated by a covariance function $k(z, \tilde{z})$ to characterize the connection between the function values at different reconstructed points. We adopt a squared exponential covariance function with the property of infinite differentiability suitable for reconstructing the shape of the function, which is given by proposed by Seikel *et al.*,[97] $k(z,\tilde{z}) = \sigma_f^2 \exp\left[-\frac{(z-\tilde{z})^2}{2l^2}\right]$, where σ_f and l are the hyperparameters need to optimize the values.

We use public python package GaPP[b] to calibrate the GRB relation from the SNe Ia. We use the J221 GRB data[c], and the Pantheon+ sample[95] comprising 1701 light curves of 1550 unique spectroscopically confirmed SNe Ia[d]. The distance modulus μ is related to the luminosity distance d_L: $\mu = m - M = 5\log\frac{d_L}{\mathrm{Mpc}} + 25$, where m and M correspond to the apparent magnitude and absolute magnitude, respectively. The reconstructed apparent magnitudes from Pantheon+ sample are showed in Fig. 1. We find that the SNe Ia data points are sparse at $0.8 \leq z \leq 2.26$, the reconstruction function exhibits strange oscillations and large uncertainty.

To calibrate the Amati relation, we use GaPP to reconstruct the apparent magnitudes of SNe Ia data points with 39 GRBs at $z < 0.8$ from the J221 sample. In order to compare with the previous analyses,[23,35,93] we also used a subsample of SNe Ia with a redshift cutoff at $z = 1.4$ to calibrate the Amati relation with 90 GRBs at $z < 1.4$ from the J221 sample. Two likelihood function methods[104,105] are used to fit the parameters of Amati relation (a and b). The likelihood function proposed by Ref. 104 is written as

$$\mathcal{L}_{\mathrm{D}} \propto \prod_{i=1}^{N_1} \frac{1}{\sigma^2} \times \exp\left[-\frac{[y_i - y(x_i, z_i; a, b, M)]^2}{2\sigma^2}\right]. \tag{3}$$

Here $\sigma = \sqrt{\sigma_{\mathrm{int}}^2 + \sigma_{y,i}^2 + b^2\sigma_{x,i}^2}$, σ_{int} is the intrinsic scatter of GRBs, $\sigma_y = \frac{1}{\ln 10}\frac{\sigma_{E_{\mathrm{iso}}}}{E_{\mathrm{iso}}}$, $\sigma_x = \frac{1}{\ln 10}\frac{\sigma_{E_{\mathrm{p}}}}{E_{\mathrm{p}}}$, $\sigma_{E_{\mathrm{p}}}$ is the error magnitude of E_{p}, and $\sigma_{E_{\mathrm{iso}}} = 4\pi d_L^2 \sigma_{S_{\mathrm{bolo}}}(1+z)^{-1}$ is the error magnitude of E_{iso}, where $\sigma_{S_{\mathrm{bolo}}}$ is the error magnitude of S_{bolo}. It should be noted that the use of the Ref. 104 likelihood may introduce a subjective bias on the choice of the independent variable in the analysis. The likelihood function proposed by Ref. 105 has the advantage of not requiring the arbitrary choice of an independent variable among E_p and E_{iso}, which has been used to get rid of this bias.[93,106] The Ref. 105 likelihood function can be written as[81,93]

$$\mathcal{L}_{\mathrm{R}} \propto \prod_{i=1}^{N_1} \frac{\sqrt{1+b^2}}{\sigma} \times \exp\left[-\frac{[y_i - y(x_i, z_i; a, b, M)]^2}{2\sigma^2}\right] \tag{4}$$

Here the intrinsic scatter can be calculated by $\sigma_{\mathrm{int}} = \sqrt{\sigma_{y,\mathrm{int}}^2 + b^2\sigma_{x,\mathrm{int}}^2}$, in which $\sigma_{x,\mathrm{int}}$ and $\sigma_{y,\mathrm{int}}$ are the intrinsic scatter along the x-axis and y-axis.

[b] `https://github.com/astrobengaly/GaPP`

[c] We revisited the J221 sample,[92] which consists of 49 GRBs from Fermi catalog, 33 GRBs from Ref. 38 and 139 GRBs from Ref. 22.

[d] The Pantheon+ sample[95] do not use SNe from SNLS at $z > 0.8$ due to sensitivity to the U band in model training, so the Pantheon+ statistics between $0.8 < z < 1.0$ are lower than that of Pantheon[2] and the Joint Light-curve Analysis (JLA[103]).

We used the python package `emcee`[107] , which is optimized on the basis of the Metropolis-Hastings algorithm, to implement the MCMC numerical fitting method. The parameters a, b, $\sigma_{\rm int}$, and the absolute magnitude M of SNe Ia simultaneously using the MCMC method with the likelihood functions from the J221 sample with redshift $z < 0.8$ (39 GRBs) and $z < 1.4$ (90 GRBs) are shown in Table 1. We find that the fitting results of the intercept (a) with the two likelihood function methods[104, 105] are consistent in 1σ uncertainty; however, there is a significant difference in the slope parameter b with the two likelihood function methods[104, 105] . As pointed out in Ref. 93, this discrepancy arises because the likelihood employed by Ref. 104 may introduce subjective biases.To avoid any bias in the selection of independent variables, we utilize the calibration results obtained through the likelihood method proposed by Ref. 105 to construct the GRB Hubble diagrams.

Table 1. Calibration results (the intercept a, the slope b, the intrinsic scatter $\sigma_{\rm int}$ and the absolute magnitude M) of the Amati relation in the J221 GRB sample at $z < 0.8$, $z < 1.4$ by the likelihood method Reichart 2001[105] and the likelihood method D'Agostini 2005.[104]

Methods	data sets	a	b	$\sigma_{\rm int}$	M
D'Agostini 2005	39GRBs ($z < 0.8$)	$52.75^{+0.58}_{-0.58}$	$1.50^{+0.13}_{-0.13}$	0.431	$-19.50^{+0.14}_{-0.14}$
	90GRBs($z < 1.4$)	$52.83^{+0.58}_{-0.58}$	$1.59^{+0.10}_{-0.10}$	0.433	$-19.50^{+0.14}_{-0.14}$
Reichart 2001	39GRBs ($z < 0.8$)	$52.80^{+0.47}_{-0.87}$	$1.808^{+0.094}_{-0.12}$	0.413	$-19.40^{+0.14}_{-0.14}$
	90GRBs($z < 1.4$)	$52.87^{+0.58}_{-0.58}$	$2.026^{+0.083}_{-0.093}$	0.423	$-19.50^{+0.14}_{-0.14}$

3. THE HUBBLE DIAGRAM AND CONSTRAINS ON COSMOLOGICAL MODELS

We construct the Hubble diagram by extrapolating the calibration results of the Amati relation at low-redshift GRBs to high-redshift. The Hubble diagram with J221 sample are plotted in Fig. 2. The cosmological parameters can be fitted by minimizing the χ^2 statistic.

$$\chi^2_{\rm GRB} = \sum_{i=1}^{N_1} \left[\frac{\mu_{\rm obs}(z_i) - \mu_{\rm th}(z_i; p, H_0)}{\sigma_{\mu_i}} \right]^2 . \tag{5}$$

Here, $N_1 = 182$ or 131 represents the number of high-redshift GRBs with $z \geq 0.8$ or $z \geq 1.4$, respectively, in the J221 sample, $\mu_{\rm obs}$ is the observational value of distance modulus and its error σ_{μ_i}. The uncertainty of GRB distance modulus with the Amati relation is

$$\sigma^2_\mu = \left(\frac{5}{2} \sigma_{\log \frac{E_{\rm iso}}{1\rm erg}} \right)^2 + \left(\frac{5}{2\ln 10} \frac{\sigma_{S_{\rm bolo}}}{S_{\rm bolo}} \right)^2 , \tag{6}$$

where

$$\sigma^2_{\log \frac{E_{\rm iso}}{1\rm erg}} = \sigma^2_{\rm int} + \left(\frac{b}{\ln 10} \frac{\sigma_{E_{\rm p}}}{E_{\rm p}} \right)^2 + \sum \left(\frac{\partial_y(x; \theta_c)}{\partial \theta_i} \right)^2 C_{ii} \, . \tag{7}$$

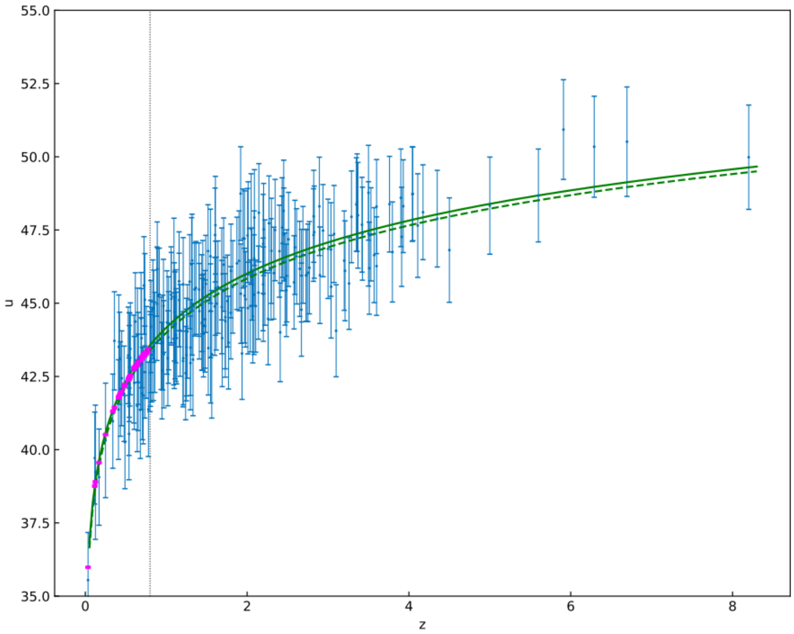

Fig. 2. GRB Hubble diagram with the J221 data set. GRBs at $z < 0.8$ were obtained by a Gaussian process from the SNe Ia data (purple points), while GRBs with $z \geq 0.8$ (blue points) were obtained by the Amati relation and calibrated with J221 at $z < 0.8$. The solid green curve presents the best-fit values from Plank CMB data at high-redshift: $H_0 = 67.36$ km s^{-1} Mpc^{-1}, $\Omega_m = 0.315$,[96] and the green long dotted curve presents the best-fit constraints on the ΛCDM model from the Pantheon+: $H_0 = 73.4$ km s^{-1}, Mpc^{-1}, $\Omega_m = 0.306$.[95, 108, 109] The black dotted line denotes $z = 0.8$.

Here $\theta_c = \{\sigma_{\rm int}, a, b\}$, and C_{ii} means the diagonal element of the covariance matrix of these fitting coefficients. $\mu_{\rm th}$ is the theoretical value of distance modulus calculated from the cosmological model, H_0 is the Hubble constant, p represents the cosmological parameters. Considering a flat space, for the wCDM model which has a constant equation of state of dark energy, the theoretical value of the luminosity distance can be obtained from

$$d_{L;\rm th} = \frac{c(1+z)}{H_0} \int_0^z \frac{dz}{[\Omega_{\rm m}(1+z)^3 + \Omega_\Lambda(1+z)^{3(1+w)}]^{\frac{1}{2}}}. \tag{8}$$

Here c is the speed of light, and $\Omega_{\rm m}$ and Ω_Λ are the present dimensionless density parameters of matter and dark energy, respectively, which satisfy $\Omega_{\rm m} + \Omega_\Lambda = 1$. For the flat ΛCDM model, $w = -1$.

We employ the Python package `emcee`[107] to constrain cosmological models with the GRB data at high-redshift. The results of 182 and 131 GRBs in the J221 data set at $z \geq 0.8$ and $z \geq 1.4$ are shown in Figures 3 (ΛCDM model) and Figure 4 (wCDM model), respectively. Constraint results with 1σ confidence level are summarized in

Tab. 2. [e]

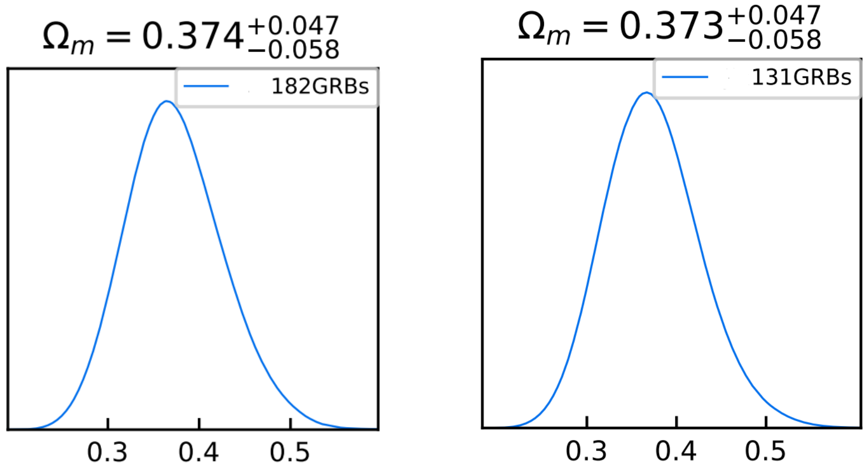

Fig. 3. Constraints on Ω_m in the ΛCDM model at redshift $z \geq 0.8$ and $z \geq 1.4$,with 182 GRBs (left panel) and 131 GRBs (right panel), respectively from J221 GRBs dataset. H_0 is set to be 70 km $s^{-1}Mpc^{-1}$ for the cases only with GRBs.

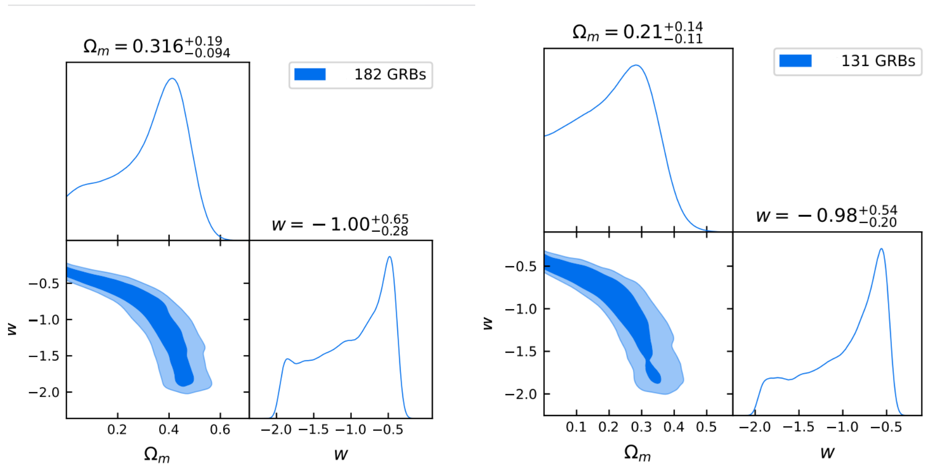

Fig. 4. Constraints on Ω_m and w in the wCDM model at redshift $z \geq 0.8$ and $z \geq 1.4$,with 182 GRBs (left panel) and 131 GRBs (right panel), respectively from J221 GRBs dataset. H_0 is set to be 70 km $s^{-1}Mpc^{-1}$ for the cases only with GRBs.

[e] It should be noted that GRB data alone are unable to constrain H_0 because of the degeneracy between H_0 and the correlation intercept parameter; therefore H_0 is set to be 70 km $s^{-1}Mpc^{-1}$ for GRB-only analyses in previous works.[?, 35, 44, 93]

In our analysis, we also use the latest OHD in Ref. 93 to constrain cosmological models, including the 31 Hubble parameter measurements at $0.07 < z < 1.965$,[110–115] and a new point at $z = 0.80$ proposed by Jiao *et al.*[116] in a similar approach. It should be noted that Borghi *et al.*[117] obtained another new OHD at $z = 0.75$. Considering these two measurements[116,117] are not fully independent and their covariance is not clear, we only use the point in Ref. 116, which taking advantage of the $1/\sqrt{2}$ fraction of systematic uncertainty. One could either use the data in Ref. 117 alternatively with other 31 OHD to investigate cosmology.[42,91,118,119] For the OHD data set, the χ^2 has the form

$$\chi^2_{\rm OHD} = \sum_{i=1}^{N_3} \left[\frac{H_{\rm obs}(z_i) - H_{\rm th}(z_i; p, H_0)}{\sigma_{H_i}} \right]^2 . \tag{9}$$

Here $N_3 = 32$ denotes the number of the Hubble parameter measurements. The total χ^2 of GRB and OHD data is

$$\chi^2_{\rm total} = \chi^2_{\rm GRB} + \chi^2_{\rm OHD}. \tag{10}$$

The constraint results of the high-redshift GRBs (182 GRBs at $z \geq 0.8$, and 131 GRBs at $z \geq 1.4$) from the J221 data set and 32 OHD, are plotted in Figures 5 (ΛCDM model) and Figure 6 (wCDM model), and summarized in Tab. 2 with the 1σ confidence level. **With 182 GRBs at $0.8 \leq z \leq 8.2$ in the J221 sample, we obtained $\Omega_{\rm m} = 0.373^{+0.047}_{-0.058}$ (ΛCDM) and $\Omega_{\rm m} = 0.316^{+0.19}_{-0.094}, w = -1.00^{+0.65}_{-0.28}$ (wCDM), which are consistent with Ref. 76 using the 3D GRB relation alone calibrated on SNe Ia ($\Omega_{\rm m} = 0.306 \pm 0.069$ for ΛCDM, fixing $h = 70$; and $w = -0.906 \pm 0.697$ for wCDM, fixing $\Omega_{\rm m} = 0.3$, $h = 70$). Our results are more stringent than previous results in Ref. 49 with the Platinum GRB and the LGRB95 sample for ΛCDM and wCDM model.** With 182 GRBs at $0.8 \leq z \leq 8.2$ in the J221 sample and 32 OHD, we obtained $\Omega_{\rm m} = 0.348^{+0.048}_{-0.066}$ and $h = 0.680^{+0.029}_{-0.029}$ for the flat ΛCDM model, and $\Omega_{\rm m} = 0.318^{+0.067}_{-0.059}$, $h = 0.704^{+0.055}_{-0.068}$, $w = -1.21^{+0.32}_{-0.67}$ for the flat wCDM model, which are consistent with the results **using the 193 GRBs (Amati relation) and SNe Ia ($\Omega_{\rm m} = 0.397 \pm 0.040$ for the ΛCDM model, and $\Omega_{\rm m} = 0.34^{+0.13}_{-0.15}, w = -0.86^{+0.36}_{-0.38}$ for the wCDM model; fixing $h = 0.6774$) at the 2σ level;[38] and the result in Ref. 74 combining SNe Ia and GRBs with a 3D optical Dainotti correlation for a flat ΛCDM cosmology** ($\Omega_{\rm m} = 0.299 \pm 0.009$). With 131 GRBs at $1.4 \leq z \leq 8.2$ in the J221 sample and 32 OHD, we obtained $\Omega_{\rm m} = 0.314^{+0.046}_{-0.063}$ and $h = 0.681^{+0.029}_{-0.029}$ for the flat ΛCDM model, and $\Omega_{\rm m} = 0.269^{+0.10}_{-0.055}$, $h = 0.683^{+0.042}_{-0.072}$, $w = -1.00^{+0.63}_{-0.29}$ for the flat wCDM model at the 1σ confidence level, which are consistent with **our previous analyses with 98 GRBs at $1.4 < z \leq 8.2$ in the A118 sample and OHD ($\Omega_{\rm m}$=$0.346^{+0.048}_{-0.069}$, h=$0.677^{+0.029}_{-0.029}$ for the flat ΛCDM model, and $\Omega_{\rm m}$=$0.314^{+0.072}_{-0.055}$, h=$0.705^{+0.055}_{-0.069}$, w=$-1.23^{+0.33}_{-0.64}$ for the flat wCDM model)[35]**.

Finally, we also use the J221 data set to constrain the ΛCDM and wCDM models by using the method of simultaneous fitting, in which the parameters of cosmological models ($\Omega_{\rm m}$, h, and w) and the relation parameters (a and b) are

Table 2. Constraints on the ΛCDM and wCDM Models at the 1σ Confidence Level from J221 GRBs at high redshift $z \geq 0.8$(182 GRBs), and $z \geq 1.4$(131 GRBs) with 32 OHD Data Sets. (For the cases only with GRBs, h is set to be 0.7.)

Models	data sets	Ω_m	h	w
ΛCDM	182 GRBs ($z \geq 0.8$)	$0.374^{+0.047}_{-0.058}$	–	–
	131 GRBs ($z \geq 1.4$)	$0.373^{+0.047}_{-0.058}$	–	–
	182 GRBs+OHD	$0.348^{+0.048}_{-0.066}$	$0.680^{+0.029}_{-0.029}$	–
	131 GRBs+OHD	$0.314^{+0.046}_{-0.063}$	$0.681^{+0.029}_{-0.029}$	–
wCDM	182 GRBs ($z \geq 0.8$)	$0.316^{+0.19}_{-0.094}$	–	$-1.00^{+0.65}_{-0.28}$
	131 GRBs ($z \geq 1.4$)	$0.21^{+0.14}_{-0.11}$	–	$-0.98^{+0.54}_{-0.20}$
	182 GRBs +OHD	$0.318^{+0.067}_{-0.059}$	$0.704^{+0.055}_{-0.068}$	$-1.21^{+0.32}_{-0.67}$
	131 GRBs +OHD	$0.269^{+0.10}_{-0.055}$	$0.683^{+0.042}_{-0.072}$	$-1.00^{+0.63}_{-0.29}$

fitted simultaneously. The results from the J221 sample combined with the OHD data set are shown in Fig. 7, and summarized in Table 3 with the 1σ confidence level. It is found that the values of the coefficients of the Amati relation (a, b, σ_int) for the flat ΛCDM model and the flat wCDM model in simultaneous fitting are almost identical, which are consistent with the results calibrating from the low-redshift data. **Compared to the results of Ref. 75 from GRBs+BAOs with EV ($\Omega_\mathrm{m} = 0.286 \pm 0.015$, $H_0 = 67.219 \pm 1.050$ km s^{-1}Mpc^{-1}), Ref. 76 from SNe Ia+BAO+GRBs using GRBs with the correction for the evolution indicated with EV ($\Omega_\mathrm{m} = 0.310 \pm 0.007$, $H_0 = 67.83 \pm 0.16$ km s^{-1}Mpc^{-1}; and $w = -1.017 \pm 0.015$ for wCDM, fixing $\Omega_\mathrm{m} = 0.3$, $h = 0.70$), and Ref. 48 from GRBs+BAOs ($\Omega_\mathrm{m} = 0.299^{+0.016}_{-0.018}$, $H_0 = 69.4 \pm 1.81$ km s^{-1}Mpc^{-1}), we find the result of h with J221+OHD for a flat ΛCDM cosmology are consistent with Ref. 75, 76 and Ref. 48 at the 1σ confidence level; and the result of Ω_m is slightly different with Ref. 75, 76 and Ref. 48 at the 1σ confidence level. We also find that the value of w for a flat wCDM model with Jia221+OHD are consistent with Ref. 76 at the 1σ confidence level. Following the same approach as in Ref. 74, 75, 77, 78, we also consider the selection biases and redshift evolution for the J221 sample, and find that the fitting results of the cosmological parameters with and without correcting for the evolutionary effects for GRBs are almost identical.**

Table 3. Simultaneous Fitting Results of Ω_m, h, a, b and σ_int in the ΛCDM and wCDM Models, with J221 GRB + 32 OHD Data Sets.

Models	Data Sets	Ω_m	h	w	a	b	σ_int
ΛCDM	J221 GRB + 32 OHD	$0.395^{+0.054}_{-0.078}$	$0.651^{+0.030}_{-0.030}$	-	$52.869^{+0.035}_{-0.035}$	$1.453^{+0.064}_{-0.064}$	$0.393^{+0.019}_{-0.022}$
wCDM	J221 GRB + 32 OHD	$0.350^{+0.11}_{-0.069}$	$0.648^{+0.037}_{-0.061}$	$-0.97^{+0.63}_{-0.30}$	$52.871^{+0.036}_{-0.036}$	$1.450^{+0.064}_{-0.064}$	$0.393^{+0.020}_{-0.023}$

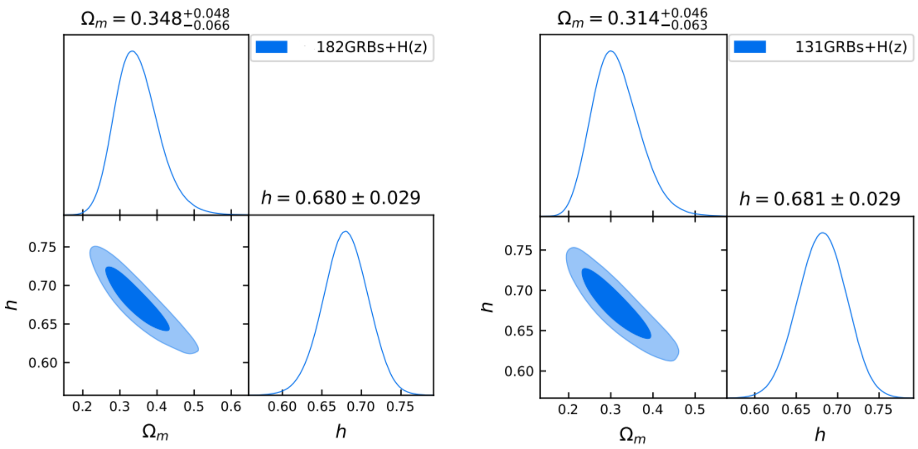

Fig. 5. Joint constraints on parameters of Ω_m and h in the ΛCDM model at redshift $z \geq 0.8$ and $z \geq 1.4$,with 182 GRBs + 32 OHD (left panel) and 131 GRBs + 32 OHD (right panel), respectively from J221 GRBs dataset.

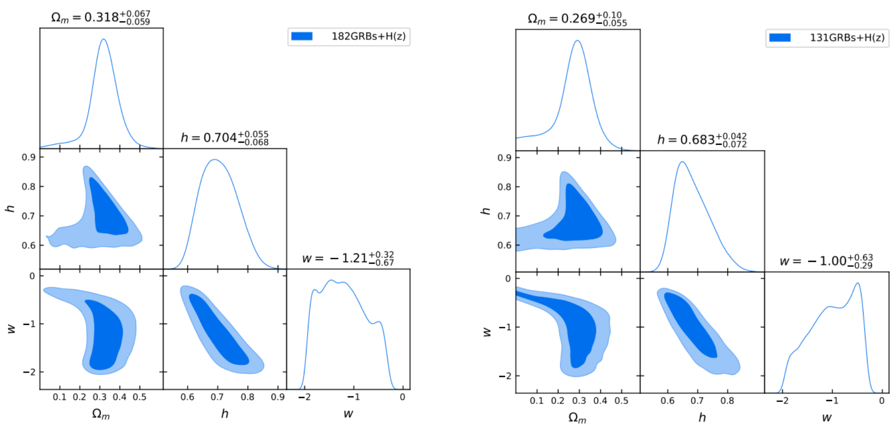

Fig. 6. Joint constraints on parameters of Ω_m and h in the ΛCDM model at redshift $z \geq 0.8$ and $z \geq 1.4$,with 182 GRBs + 32 OHD (left panel) and 131 GRBs + 32 OHD (right panel), respectively from J221 GRBs dataset.

4. SUMMARY AND DISCUSSION

In this paper, we use the Gaussian process to calibrate the Amati relation of GRBs from the Pantheon+ sample[95] by Gaussian process and obtain the GRB Hubble diagram with the latest J221 GRB sample.[92] With 131 GRBs at $1.4 \leq z \leq 8.2$ in the J221 sample and 32 OHD, we obtained $\Omega_{\rm m} = 0.314^{+0.046}_{-0.063}$ and $h = 0.681^{+0.029}_{-0.029}$ for the flat ΛCDM model, and $\Omega_{\rm m} = 0.269^{+0.10}_{-0.055}$, $h = 0.683^{+0.042}_{-0.072}$, $w = -1.00^{+0.63}_{-0.29}$

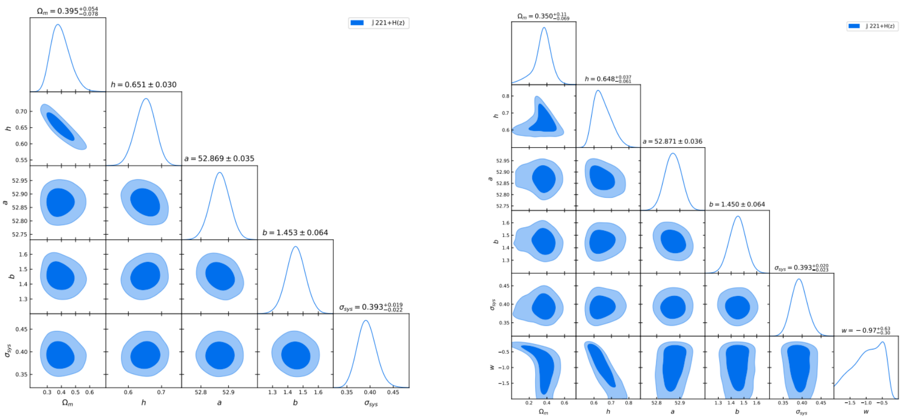

Fig. 7. Simultaneous fitting parameters of Ω_m, h, a, b and σ_{int} in the ΛCDM model with J221 GRBs + 32 OHD (left panel), and Ω_m, h, a, b, σ_{int} and w in the wCDM model with J221 GRBs + 32 OHD (left panel) (right panel).

for the flat wCDM model at the 1σ confidence level. We find that our results with 131 GRBs at $1.4 \leq z \leq 8.2$ are consistent with previous analyses that obtained in Ref. 35. We also use GRB data sets of J221 sample to fit $\Omega_{\rm m}$, h, a, b, $\sigma_{\rm int}$ and w parameters simultaneously. It is found that the simultaneous fitting results are consistent with those obtained from the low-redshift calibration method.

H_0 with a redshift evolving is an interesting idea for the H_0 tension.[120–125] Recently, **Dainotti *et al.*[120,121] fit the H_0 values with a function mimicking the redshift evolution to find a slowly decreasing trend.** Jia *et al.*[123] find a decreasing trend in the Hubble constant with a significance of a 5.6σ confidence level with SN Ia, OHD and baryon acoustic oscillation (BAO) data, which indicate that H_0 value is consistent with that measured from the local data at low redshift and drops to the value measured from the CMB at high redshift. Malekjani *et al.*[125] find the evolving (H_0,$\Omega_{\rm m}$) values above $z = 0.7$ in Pantheon+ sample. We find that the H_0 value with GRBs at $0.8 \leq z \leq 8.2$ and OHD at $z \leq 1.975$ seems to favor the one from the Planck observations, and the $\Omega_{\rm m}$ value of our results for the flat ΛCDM model is consistent with the CMB observations at the 1σ confidence level. A larger $\Omega_{\rm m}$ values in the ΛCDM model with GRBs at high redshift is obtained, but adding OHD at low redshift removes this trend.

It should be note that the potential use of machine learning (ML) algorithms for reconstructing light curves could further enhance parameter determination.[126] Dainotti *et al.*[127] use ML to infer redshifts from the observed temporal and spectral features of GRBs. Moreover, ML have been use to calibrate the Amati relation.[40,128] Furthermore, Dainotti *et al.*[74,121] investigate perspective of the future contribution of GRB-Cosmology. In future, GRBs could be used to set tighter constraints on cosmological models with the GRB sample from Fermi data with much smaller scatters, as well as the data from the Chinese-French mission SVOM (the Space-based multi-band astronomical Variable Objects Monitor),[129] which will provide a substantial enhancement of the number of GRBs with measured redshift and spectral parameters.

ACKNOWLEDGMENTS

We thank Guangzhen Wang, Zhiguo Xiong and Prof. Puxun Wu for for discussions and kind help. We also thank the referee for helpful comments and constructive suggestions. This project was supported by the Guizhou Provincail Science and Technology Foundation (QKHJC-ZK[2021] Key 020).

References

1. Cucchiara, A., Levan, A., Fox, D. B., *et al. Astrophys. J.* **736** (2011) 7.
2. Scolnic, D. M., Jones, D. O., Rest, A., *et al. Astrophys. J.* **859** (2018) 101.
3. Fenimore, E. E., & Ramirez-Ruiz, E., *preprint astro-ph/0004176* (2000).
4. Norris, J. P., Marani, G. F., & Bonnell, J. T., *Astrophys. J.* **534** (2000) 248.
5. Amati, L., Frontera, F., Tavani, M., *et al.*, *Astron. Astrophys.* **390** (2000) 81.
6. Ghirlanda, G., Ghisellini, G., & Lazzati, D., *Astrophys. J.* **616** (2004) 331.
7. Yonetoku, D., Murakami, T., Nakamura, T., *et al.*, *Astrophys. J.* **609** (2004) 935.
8. Liang, E., & Zhang, B., *Astrophys. J.* **633** (2005) 611.
9. Firmani, C., Ghisellini, G., Avila-Reese, V., & Ghirlanda, G., *Mon. Not. R. Astron. Soc.* **370** (2006) 185.
10. Ghirlanda, G., Ghisellini, G.,& Firmani, C., *New J. Phys* **8** (2006) 123.
11. Schaefer, B. E., *Astrophys. J.* **660** (2007) 16.
12. Tsutsui, R., Nakamura, T., Yonetoku, D., Murakami, T., Kodama, Y., & Takahashi, K., *J. Cosmol. Astropart. Phys.* **0908** (2009) 015.
13. Izzo, L., Muccino, M., Zaninoni, E., Amati, L., & Della Valle, M., *Astron. Astrophys.* **582** (2015) A115.
14. Dai, Z., Liang, E., & Xu, D., *Astrophys. J.* **612** (2004) L101.
15. Liang, N., Xiao, W. K., Liu, Y., & Zhang, S. N., *Astrophys. J.* **685** (2008) 354.
16. Capozziello, S., & Izzo, L., *Astron. Astrophys.* **490** (2008) 31.
17. Capozziello, S. & Izzo, L., *Nucl. Phys. Proc. Suppl.* **194** (2009) 206.
18. Wei, H., Zhang, S. N., *Eur. Phys. J.* **63** (2009) 139.
19. Wei, H., *J. Cosmol. Astropart. Phys.* **08** (2010) 020.
20. Liang, N., Wu, P., & Zhang, S. N., *Phys. Rev. D* **81** (2010) 083518.
21. Liang, N., Xu, L., & Zhu, Z. H., *Astron. Astrophys.* **527** (2011) A11.
22. Wang, J. S., Wang, F. Y., Cheng, K. S., & Dai, Z. G., *Astron. Astrophys.* **585** (2016) A68.
23. Liu, Y., Liang, N., Xie, X., *et al.*, *Astrophys. J.* **935** (2022) 7.
24. Liang, N., & Zhang, S., *AIP Conf. Proc.* Vol. 1065 (2008).
25. Kodama, Y., Yonetoku, D., Murakami, T., *et al.*, *Mon. Not. R. Astron. Soc.* **391** (2008) L1.
26. Capozziello, S., & Izzo, L., *Astron. Astrophys.* **519** (2010) A73.
27. Gao, H., Liang, N., & Zhu, Z.-H., *Int. J. Mod. Phys. D.* **21** (2011) 1250016.
28. Liu, J., & Wei, H., *Gen. Rel. Grav.* **47** (2015) 141.

29. Demianski, M., Piedipalumbo, E., Sawant, D., & Amati, L., *Astron. Astrophys.* **598** (2017) A112.
30. Demianski, M., Piedipalumbo, E., Sawant, D., & Amati, L., *Mon. Not. R. Astron. Soc.* **506** (2021) 903.
31. Shirokov, S. I., Sokolov, I. V., Lovyagin, N. Y., *et al.*, *Mon. Not. R. Astron. Soc.* **496** (2020) 1530.
32. Muccino, M., Izzo, L., Luongo, O., *et al.*, *Astrophys. J.* **908** (2021) 181.
33. Lovyagin, N. Y., Gainutdinov, R. I., Shirokov, S. I., *et al.*, *Universe* **08** (2022) 334.
34. Tang L., Lin, H.-N., Li X., & Liu L., *Mon. Not. R. Astron. Soc.* **509** (2022) 1194.
35. Liang, N., Li, Z., Xie, X., & Wu, P., *Astrophys. J.* **941** (2022) 84.
36. Jimenez, R., & Loeb, A., *Astrophys. J.* **573** (2002) 37.
37. Jimenez, R., Verde, L., Treu, T. & Stern, D., *Astrophys. J.* **593** (2003) 622.
38. Amati, L., D'Agostino, R., Luongo, O., Muccino, M., & Tantalo, M., *Mon. Not. R. Astron. Soc.* **486** (2019) L46.
39. Montiel, A., Cabrera, J. I., & Hidalgo, J. C., *Mon. Not. R. Astron. Soc.* **501** (2021) 3515.
40. Luongo, O., & Muccino, M., *Mon. Not. R. Astron. Soc.* **503** (2021) 4581.
41. Luongo, O., & Muccino, M., *Mon. Not. R. Astron. Soc.* **518** (2023) 2247.
42. Muccino, M., Luongo, O., & Jain, D., *Mon. Not. R. Astron. Soc.* **523** (2023) 4938.
43. Amati, L., Guidorzi, C., Frontera, F., *et al.*, *Mon. Not. R. Astron. Soc.* **391** (2008) 577.
44. Khadka, N., Luongo, O., Muccino, M., & Ratra, B., *J. Cosmol. Astropart. Phys.* **091** (2021) 042.
45. Khadka, N. & Ratra, B., *Mon. Not. R. Astron. Soc.* **499** (2020) 391.
46. Fana Dirirsa, F., Razzaque, S., Piron, F., *et al.*, *Astrophys. J.* **887** (2019) 19.
47. Cao, S., Khadka, N., & Ratra, B., *Mon. Not. R. Astron. Soc.* **510** (2022) 2928.
48. Cao, S., Dainotti, M., & Ratra, B., *Mon. Not. R. Astron. Soc.* **512** (2022) 439.
49. Cao, S., Dainotti, M., & Ratra, B., *Mon. Not. R. Astron. Soc.* 516 (2022) 1386.
50. Dainotti, M. G., Cardone V. F., & Capozziello S., *Mon. Not. R. Astron. Soc.* 391 (2008) L79.
51. Cardone, V. F., Capozziello, S., & Dainotti, M. G., *Mon. Not. R. Astron. Soc.* 400 (2009) 775.
52. Cardone V. F., Dainotti, M. G., Capozziello, S., & Willingale, R. *Mon. Not. R. Astron. Soc.* 408 (2010) 1181.
53. Dainotti, M. G., Cardone V. F., & Capozziello S., *Astrophys. J.* 722 (2010) L215.
54. Dainotti, M. G., Ostrowski, M., & Willingale, R. *Mon. Not. R. Astron. Soc.* 418 (2011) 2202.
55. Dainotti, M. G., Cardone, V. F., Capozziello, S., *et al.* *Astrophys. J.* 730 (2011) 135.
56. Dainotti, M. G., Petrosian, V., Singal, J., *et al.* *Astrophys. J.* 774 (2013) 157.
57. Dainotti, M. G., Cardone, V. F., Piedipalumbo, E., *et al.* *Mon. Not. R. Astron. Soc.* 436 (2013) 82.
58. Dainotti, M. G., Petrosian, V., Willingale, R., *et al.* *Mon. Not. R. Astron. Soc.* 451 (2015) 3898.
59. Dainotti, M. G., Del Vecchio, R., Shigehiro, N., *et al.* *Astrophys. J.* 800 (2015) 31.
60. Dainotti, M. G., Postnikov, S., Hernandez, X., *et al.* *Astrophys. J.* 825

(2016) L20
61. **Del Vecchio, R., Dainotti, M. G., & Ostrowski, M. *et al. Astrophys. J.* 828 (2016) 36.**
62. **Dainotti, M. G., Nagataki, S., Maeda, K., *et al. Astron. Astrophys.* 600 (2017) 98.**
63. **Dainotti, M. G., Hernandez, X., Postnikov, S.,*et al. Astrophys. J.* 848 (2017) 88.**
64. **Srinivasaragavan, G. P., Dainotti, M. G., Fraija, N. Fraija *et al. Astrophys. J.* 903 (2020) 18.**
65. **Dainotti, M. G., Lenart, A. L., Sarracino, G., *et al. Astrophys. J.* 904 (2020) 97.**
66. **Dainotti, M. G., Livermore, S., Kann, D. A., *et al. Astrophys. J.* 905 (2020) L26.**
67. **Dainotti, M. G., Lenart, A. L., Fraija, N., *et al. PASJ* 73 (2021) 970.**
68. **Levine, D., Dainotti, M., Zvonarek, K. J., *et al. Astrophys. J.* 925 (2021) 15.**
69. **Tian, X., Li, J.-L., Yi, S. X., *et al. Astrophys. J.* 958 (2023) 74.**
70. **Hu, J. P., Wang, F. Y., & Dai, Z. G., *Mon. Not. R. Astron. Soc.* 507 (2021) 730.**
71. **Wang, F. Y., Hu, J. P., Zhang, G. Q., & Dai, Z. G., *Astrophys. J.* 924 (2022) 97.**
72. **Li, J.-L., Yang, Y.-P., Yi, S.-X., Hu, J.-P., Wang, F.-Y., & Qu, Y.-K., *Astrophys. J.* 953 (2023) 58.**
73. Dainotti, M. G., Young, S., Li, L., *et al.*, *Astrophys. J. Suppl.* **261** (2022) 25.
74. **Dainotti, M. G., Nielson, V., Sarracino, G., *et al.*, *Mon. Not. R. Astron. Soc.* 514 (2022) 1828.**
75. **Dainotti, M. G., Sarracino G., & Capozziello S., *PASJ* 74 (2022) 1095.**
76. **Dainotti, M. G., Lenart, A. L., Chraya, A., *et al.*, *Mon. Not. R. Astron. Soc.* 518 (2023) 2201.**
77. **Dainotti, M. G., Bargiacchi, G., & Bogdan, M. *et al.*, *Astrophys. J.* 951 (2023) 63.**
78. **Bargiacchi, G., Dainotti, M. G., Nagataki, S.,*et al. Mon. Not. R. Astron. Soc.* 521 (2023) 3909.**
79. **Bargiacchi, G., Dainotti, M. G., & Capozziello, S. *Mon. Not. R. Astron. Soc.* 525 (2023) 3104.**
80. Basilakos, S., & Perivolaropoulos., L. *Mon. Not. R. Astron. Soc.* **391** (2008) 411.
81. Lin, H. N., Li, X. & Chang, Z., *Mon. Not. R. Astron. Soc.* **455** (2016) 2131.
82. Wang, G. J., Yu, H., Li, Z. X., Xia, J. Q., & Zhu Z.-H., *Astrophys. J.* **836** (2017) 103.
83. Dai, Y., Zheng, X.-G., Li, Z. X., *et al.*, *Astron. Astrophys.* **651** (2000) L8.
84. Tang L., Li X., Lin, H.-N., & Liu L., *Astrophys. J.* **907** (2021) 121.
85. **Petrosian, V., Kitanidis, E., & Kocevski, D. *Astrophys. J.* 806 (2015) 44.**
86. **Lloyd-Ronning, N. M., Aykutalp, A., & Johnson, J. L. *Mon. Not. R. Astron. Soc.* 488 (2019) 5823.**
87. **Tsvetkova, A., Frederiks, D., Golenetskii, S., *et al. Astrophys. J.* 850 (2017) 161.**
88. **Yu, H., Wang, F. Y., Dai, Z. G. *et al. Astrophys. J. Suppl.* 218 (2015) 13.**
89. **Dainotti, M. G., Petrosian, V., & Bowden, L. *Astrophys. J.* 914 (2021) L40.**
90. Liu, Y., Chen, F., Liang, N., *et al.*, *Astrophys. J.* **931** (2022) 50.

91. Kumar, D. et al., *et al.*, *J. Cosmol. Astropart. Phys.* **07** (2023) 021.
92. Jia, X. D., Hu, J. P., Yang, J., Zhang, B. B., & Wang, F. Y., *Mon. Not. R. Astron. Soc.* **516** (2022) 2575.
93. Li, Z., Zhang, B., & Liang, N., *Mon. Not. R. Astron. Soc.* **521** (2023) 4406.
94. Mu, Y., Chang, B., & Xu, L. (2023), (arXiv:2302.02559).
95. Scolnic., *et al.*, *Astrophys. J.* **938** (2022) 113.
96. Plank Collaboration. Aghanim, N., Akrami, Y., Arroja, F., *et al.*, *Astron. Astrophys.* **641** (2020) A1.
97. Seikel, M., Clarkson, C., & Smith, M., *J. Cosmol. Astropart. Phys.* **06** (2012) 036.
98. Seikel, M., Yahya, S., Maartens, R., & Clarkson, C. , *Phys. Rev. D* **86** (2012) 083001.
99. Lin, H. N., Li, M. H., & Li, X., *Mon. Not. R. Astron. Soc.* **480** (2018) 3117.
100. Li, X., Keeley, R. E., Shafieloo, A., *et al.*, *Mon. Not. R. Astron. Soc.* **507** (2021) 919.
101. Sun, W., Jiao, K., & Zhang, T.-J., *Astrophys. J.* **915** (2021) 123.
102. Benisty, D., Mifsud, J., Levi Said, J., & Staicova, D., *Physics of the Dark Universe* **39** (2023) 101160.
103. Betoule, M., Kessler, R., Guy, J., *et al.*, *Astron. Astrophys.* **568** (2014) A22.
104. D'Agostini, G., (2005)(arXiv: physics/0511182)
105. Reichart, D. E., *Astrophys. J.* **553** (2001) 57.
106. Amati, L. & Della Valle, *Int. J. Mod. Phys. D.* **22** (2013) 1330028.
107. Foreman-Mackey, D., Hogg, D. W., Lang, D., & Goodman, J., *Publications of the Astronomical Society of the Pacific* **125** (2013) 306.
108. Brout, D., Scolnic, D., *et al.*, *Astrophys. J.* **938** (2022) 110.
109. Riess, A. G., Yuan, W., Macri, L. M., *et al.*, *Astrophys. J.* **934** (2022) L7.
110. Stern, D., Jimenez, R., Verde, L., Kamionkowski, M. & Starford, S. A., *J. Cosmol. Astropart. Phys.* **02** (2010) 008.
111. Moresco, M., Verde, L., Pozzetti, L., Jimenez, R. & Cimatti, A., *J. Cosmol. Astropart. Phys.* **08** (2012) 006.
112. Moresco, M., *Mon. Not. R. Astron. Soc.* **450** (2015) L16.
113. Moresco, M., Pozzetti, L., Cimatti, A., *et al.*, *J. Cosmol. Astropart. Phys.* **05** (2016) 014.
114. Zhang, C., Zhang, H., Yuan, S., Liu, S., Zhang, T. & Sun, Y., *Res. Astron. Astrophys* **14** (2014) 1221.
115. Ratsimbazafy, A. L., Loubser, S. I., Crawford, S. M., *et al.*, *Mon. Not. R. Astron. Soc.* **467** (2017) 3239.
116. Jiao, K., Borghi, N., Moresco, M. & Zhang, T-J., *Astrophys. J. Suppl.* **265** (2023) 48.
117. Borghi, N., Moresco, M. & Cimatti, A., *Astrophys. J.* **928** (2022) L4.
118. Lee, S., *Mon. Not. R. Astron. Soc.* **522** (2023) 3248
119. Favale, A., Gomez-Valent, A. & Migliaccio M., *Mon. Not. R. Astron. Soc.* **523** (2023) 3406
120. Dainotti, M. G., De Simone, B., Schiavone, T., *et al.* *Astrophys. J.* 912 (2021) 50.
121. Dainotti, M. G., De Simone, B., Schiavone, T., *et al.* *Galaxies* 10 (2022) 24.
122. Colgain, E. O., Sheikh-Jabbari, M. M., Solomon, R. *et al.* *Phys. Rev. D.* 106 (2022), L041301.
123. Jia, X. D., Hu, J. P., & Wang, F. Y., *Astron. Astrophys.* **674** (2023) A45.
124. Hu, J. P., & Wang, F. Y., *Universe* **9(2)** (2023) 94
125. Malekjani, M., Mc Conville, R., Colgain, E. O. *et al.* (2023), arXiv:2301.12725.
126. Dainotti, M. G., Sharma, R., Narendra, A., *et al.* *Astrophys. J. Suppl.*

267 (2023) 42.
127. **Dainotti, M. G., Petrosian, V., Bogdan, M. *et al.* (2019), arXiv:1907.05074**
128. **Zhang, B., Xie., X. Y., Nong, X. D. *et al.* (2023), arXiv:2312.09440**
129. Bernardini, M. G., Cordier, B. & Wei., J., *Galaxies* **9** (2021) 113.